Title

TAUTOMERISM IN XENON HEXAFLUORIDE: AN INVESTIGATION OF XENON HEXAFLUORIDE AND ITS COMPLEXES BY RAMAN SPECTROSCOPY

Authors

Adams, Chris J.
Bartlett, Neil.

Publication Date

1977-12-01

Submitted to Israel Journal of Chemistry
(In Press)

LBL-3136
Preprint

TAUTOMERISM IN XENON HEXAFLUORIDE: AN INVESTIGATION OF XENON HEXAFLUORIDE AND ITS COMPLEXES BY RAMAN SPECTROSCOPY

Chris J. Adams and Neil Bartlett

December 1977

Prepared for the U. S. Department of Energy
under Contract W-7405-ENG-48

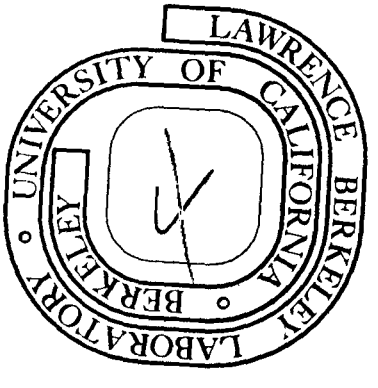

LBL-3136

DISCLAIMER

TAUTOMERISM IN XENON HEXAFLUORIDE: AN INVESTIGATION OF XENON HEXAFLUORIDE AND ITS COMPLEXES BY RAMAN SPECTROSCOPY[1]

by

Chris J. Adams[2] and Neil Bartlett*

Inorganic Materials Research Division, Lawrence Berkeley Laboratory
and Department of Chemistry, University of California
Berkeley, California 94720

ABSTRACT:

Raman spectra are reported for (i) complexes of xenon hexafluoride with the fluoride-ion acceptors BF_3, PdF_4, PF_5, AsF_5, RuF_5, PtF_5, and AuF_5, and (ii) for solutions of xenon hexafluoride in HF and in WF_6. Vibrational assignments are made for the cations XeF_5^+ and $Xe_2F_{11}^+$, and evoke a normal coordinate analysis for XeF_5^+. Xenon hexafluoride, present in concentrated solution in HF as $[XeF_5^+F^-]_4$, progressively ionizes on dilution to give $Xe_2F_{11}^+$ and XeF_5^+; on the other hand, in WF_6 solution $[XeF_5^+F^-]_4$ exists in equilibrium only with molecular XeF_6.

INTRODUCTION

A simple model predicts that the ease of removal of a fluoride ion from a xenon fluoride molecule should decrease in the order $XeF_2 > XeF_4 > XeF_6$, as the oxidation number of and positive charge on the xenon atom rise. That the actual sequence is $XeF_6 > XeF_2 > XeF_4$, was first indicated by comparative studies of reactions of the fluorides with acceptors,[3] and was later confirmed by enthalpy measurements[4] for the processes:

$$XeF_n(g) \longrightarrow XeF_{n-1}^{+}(g) + F^{-}(g) \qquad n = 2, 4, 6.$$

The anomalously high ability of xenon hexafluoride as a donor of fluoride ion distinguishes it from the hexafluorides of other elements, and cations thus derived (viz. XeF_5^+ and $Xe_2F_{11}^+$) play an important role in the chemistry of this strange and fascinating compound. Recent crystallographic studies in these laboratories have defined XeF_5^+ and $Xe_2F_{11}^+$ cations in complexes of xenon hexafluoride with Lewis acids, e.g. $[XeF_5^+][RuF_6^-]$,[5] $[XeF_5^+][AsF_6^-]$,[6] $[XeF_5^+]_2[PdF_6^{2-}]$,[7] and $[Xe_2F_{11}^+][AuF_6^-]$.[8] In these salts the XeF_5^+ cation approaches the C_{4v} geometry predicted by the valence-shell-electron-pair repulsion theory; the $Xe_2F_{11}^+$ cation comprises two XeF_5^+ units linked by a bridging fluoride ion. Furthermore, the four modifications of solid xenon hexafluoride consist of $[XeF_6]_4$ and $[XeF_6]_6$ oligomers, which are aggregates of XeF_5^+ cations and bridging fluoride anions, and which may usefully be formulated as $[XeF_5^+F^-]_4$ and $[XeF_5^+F^-]_6$.[9]

The availability of this crystallographic information on XeF_6 and a variety of its complexes, encouraged us to undertake the study reported in this paper. We had two objectives. Firstly, it was intended to

achieve a better understanding of the vibrational spectrum of the XeF_5^+ cation, which, up to the time of our study had, received scant attention. An independent study by Christe[9a] became available after our study[1] was complete. Secondly, using the Raman fingerprints obtained in this and earlier work[10,11,12] for XeF_5^+ and $Xe_2F_{11}^+$ and derived from $[XeF_5^+F^-]_4$ and molecular XeF_6 from earlier Raman data for the solid, liquid, and gaseous compound,[13,14] the nature of xenon hexafluoride in solution was undertaken. To these ends we report Raman spectra for salts of the XeF_5^+ and $Xe_2F_{11}^+$ cations, and for solutions of the hexafluoride in anhydrous hydrogen fluoride (an ionizing solvent) and in tungsten hexafluoride (a non-ionizing solvent).

EXPERIMENTAL

General

Solids were manipulated in the dry nitrogen atmosphere of a V.A.C. Dri-Lab. Volatiles were transferred using a prefluorinated Monel and Kel-F vacuum system.

Preparative

(i) Starting materials. Xenon hexafluoride was prepared from xenon and excess fluorine by the sodium fluoride complex method.[15] Hydrogen fluoride (Matheson) was fluorinated at room temperature before use. BF_3, PF_5, AsF_5, and WF_6 (all Matheson) were taken directly from the cylinder without purification. The vapours of these compounds showed no impurities detectable by infrared spectroscopy.

(ii) Complexes. $XeF_6 \cdot BF_3$,[16,17] $XeF_6 \cdot AsF_5$,[17,18] $2XeF_6 \cdot AsF_5$, and $2XeF_6 \cdot PF_5$[18] were prepared by mixing the component compounds; in each case mass balance and identification of excess reagent confirmed the composition of the compound. $XeF_6 \cdot RuF_5$,[5] $XeF_6 \cdot PtF_5$,[19] and $2XeF_6 \cdot AuF_5$[8] were from samples previously prepared for X-ray crystallographic studies. $XeF_6 \cdot AuF_5$ was made by decomposing $2XeF_6 \cdot AuF_5$ in vacuo at 110°C.[20] The purity of the samples was checked by X-ray powder photography.

Raman Spectroscopy

(i) Solid samples. Using the Dri-Lab, finely powdered solids were packed into thin-walled quartz capillaries (1 mm i.d.), which were temporarily stopped with Kel-F grease, removed from the Dri-Lab, and immediately sealed by drawing down in a small flame.

(ii) Liquid samples. Teflon-FEP or Kel-F tubes (ca. 3 mm i.d.), fitted via Swagelok couplings with Whitey valves 1KS4, were thoroughly prefluorinated, evacuated, and weighed. The solute was loaded, either using the Dri-Lab, or, in the case of xenon hexafluoride, by condensation via the (carefully prefluorinated) vacuum system; the apparatus was reweighed. Fluorination of connecting lines also preceded transfer of solvent (HF, WF_6); the tubes were then heat-sealed under dynamic vacuum, and the final weight of the tube, fittings, and contents determined. In calculating the concentrations of the solutions allowance was made for the vapor over the liquid.

(iii) Instrumental. Raman spectra were excited at 4880 Å, 6328 Å, or 6471 Å, and recorded using a Spex 1401 monochromator and a photoncounting detector system. Solids were examined using colinear-excitation-back-scattering light collection, the laser beam being brought to a slit-shaped focus on the sample. For liquids in Kel-F or FEP tubes transverse-excitation-transverse-viewing was more effective; to obtain qualitative depolarization ratios the laser beam was polarized perpendicular to the viewing axis, and the scattered radiation was analyzed before the entrance slit.

(iv) Impurity, solvent, and cell features. Raman features due to cell walls and solvent were observed: they have been identified in the figures, but omitted from the tables.

Teflon-FEP: 752 w, 732 s, 386 m, 291 m.

Kel-F: 775 vw, 670 s, 620 w, 490 b, w; 450 m, 380 b, w.

WF_6: 776 vs, p (ν_1), 671 w, dp (ν_2), 324 w, dp (ν_5), 268 vw, dp ($2\nu_6$).

A few of the solutions showed weak polarized Raman lines at 920 cm^{-1} and 570 cm^{-1} attributable to traces of $XeOF_4$; these have been identified in the figures.

X-ray crystallography

Single crystals of $XeF_6 \cdot BF_3$ were grown by vacuum sublimation in Kel-F at room temperature; single crystals of $XeF_6 \cdot AuF_5$ were grown at 100°C under 50 cm N_2. Crystal manipulation was carried out in the Dri-Lab. Crystals were lodged in narrow quartz capillaries which were subsequently sealed in the same manner as the Raman samples. Crystal data, obtained from precession photographs, are summarized in Table 3. $XeF_6 \cdot BF_3$ decomposed in the beam, and the space group could not be unambiguously determined.

The Raman samples themselves were used to obtain powder photographs by the Debye-Scherrer method.

Infrared spectroscopy

Volatile solids were sublimed from room temperature onto a silver chloride window cooled to -196°C in an evacuated cell; the infrared spectrum of the solid was recorded with a Perkin Elmer 337 Spectrometer.

RESULTS AND DISCUSSION

Complexes of xenon hexafluoride

It has been shown by X-ray crystallography that the compounds $XeF_6 \cdot AsF_5$, $XeF_6 \cdot RuF_5$, $XeF_6 \cdot PtF_5$ and 2 $XeF_6 \cdot PdF_4$ are salts of the XeF_5^+ cation; the presence of the XeF_5^+ cation in $XeF_6 \cdot BF_3$, $XeF_6 \cdot AuF_5$, and in the colorless solutions of $XeF_6 \cdot BF_3$ and $XeF_6 \cdot AsF_5$ in anhydrous HF is confirmed by the observation of a characteristic pattern of lines attributable to XeF_5^+. Similarly, the Raman spectra of 2 $XeF_6 \cdot PF_5$, 2 $XeF_6 \cdot AsF_5$ and their colorless solutions in HF strongly suggest by their resemblance to those of $[Xe_2F_{11}^+][AuF_6^-]$ that the $Xe_2F_{11}^+$ cation occurs in all cases.

(i) XeF_5^+ salts

Listed in Table 1 are the Raman and infrared frequencies recorded for solid $[XeF_5^+][BF_4^-]$ together with Raman data for the compound in solution in anhydrous hydrogen fluoride. Raman spectra of the salts with hexafluoroanions are given in Table 2. Some representative traces are shown in Figures 1 and 2.

Interpretation of the spectra begins most readily with the HF solutions of $[XeF_5^+][BF_4^-]$ and $[XeF_5^+][AsF_6^-]$. The Raman lines of BF_4^- and AsF_6^- in HF are well-known and readily identifiable;[21] the residual lines (due to XeF_5^+) were the same for both salts. The frequencies observed for XeF_5^+ varied little (± 2 cm^{-1}) over the concentration range studied (0.3 - 5.0 M). At the higher concentrations, however, the lines were much broader, and relative peak heights changed; in particular, at higher concentrations the height of the ca. 625 cm^{-1} line increases relative to that at 676 cm^{-1}. Changes in relative integrated intensities

were not investigated. We did not observe the Raman line at 450 cm^{-1} reported by Frlec et al.[12] for solutions of $[XeF_5^+][AsF_6^-]$ in HF.

The Raman spectrum of solid $[XeF_5^+][BF_4^-]$ closely resembles that of its solution in HF; anion lines are again easily identified. However, interpretation of the spectra of the solid XeF_5^+ hexafluorometallates (Table 2) is complicated by two factors. Firstly, the regions of the spectrum associated with fundamentals in Xe-F and M-F stretching modes overlap, as do the regions associated with F-Xe-F and F-M-F deformations. Secondly, crystallographic evidence shows that the cations and anions depart from their respective idealized C_{4v} and O_h geometries, and the resultant breakdown in vibrational selection rules is manifest in the splitting of degenerate fundamentals and the observation in the Raman spectrum of formally forbidden transitions. In assigning the spectra of the solids, therefore, consideration was given to the constraints placed on the vibrations of the ions by the unit cell, using the information summarized in Table 3. It was expected, furthermore, that isomorphous compounds would display similar patterns in their spectra.

The XeF_5^+ cation of C_{4v} symmetry has the vibrational representation $3a_1 + 2b_1 + b_2 + 3e$; all modes are Raman active, but only $3a_1 + 3e$ are allowed in infrared absorption. Nine Raman lines attributable to fundamentals of XeF_5^+ were observed, and assigned on the basis of their relative intensities, depolarization ratios, and by comparison with the spectra of related molecules (Table 4). The strong polarized lines at ca. 670 cm^{-1} and ca. 610 cm^{-1} are clearly ν_1 and ν_2, the a_1 stretching fundamentals. The deformations ν_3, ν_6, ν_8, and ν_9 are assigned in the same order as in IF_5.[21] The Raman line at ca. 300 cm^{-1} is probably

polarized in solution, supported its assignment as $\nu_3(\underline{a}_1)$. The splitting of the ca. 400 cm^{-1} line in several of the solids suggests that it is indeed $\nu_8(\underline{e})$. (The behavior of this fundamental exemplifies the effects of isomorphism; it is split in $[XeF_5^+][AsF_6^-]$ and $[XeF_5^+][AuF_6^-]$, but not in $[XeF_5^+][RuF_6^-]$ and $[XeF_5^+][PtF_6^-]$.) $\nu_7(\underline{e})$, the degenerate stretching mode of the basal XeF_4 unit, should generate a strong infrared absorption, and is assigned at ca. 660 cm^{-1} since the infrared spectrum of $[XeF_5^+][BF_4^-]$ has its strongest absorption at this frequency; the orthorhombic lattice of $[XeF_5^+][BF_4^-]$ forbids a four-fold axis about the xenon atom, and the Raman transition corresponding to ν_7 for this compound is in fact split. The two $\underline{b}_1$ fundamentals ν_4 and ν_5, and the $\underline{b}_2$ fundamental ν_6, are not allowed in the infrared, and by analogy with other MX_5 $\underline{C}_{4v}$ species, should give only very weak Raman lines. ν_4 is assigned at ca. 610 cm^{-1}, and in solution and in some of the solids it is obscured by the much more intense $\nu_2(\underline{a}_1)$; weak lines at ca. 240 cm^{-1} and ca. 260 cm^{-1}, observed for some of the solids, are tentatively identified as $\nu_5(\underline{b}_1)$ and $\nu_6(\underline{b}_2)$. Detailed assignments are given in Tables 1 and 2.

In Table 4 the fundamental frequencies of XeF_5^+ are compared with data for the isoelectronic molecules SbF_5^{2-}, TeF_5^-, IF_5, and $XeOF_4$. While there is a smooth increase in frequency from SbF_5^{2-} to IF_5, the fundamentals of XeF_5^+ are in some cases lower than those of IF_5; the effect is especially striking for $\nu_1(\underline{a}_1)$, which lies at 710 cm^{-1} in IF_5[22] and ca. 670 cm^{-1} in XeF_5^+. Moreover the bond lengths of XeF_5^+ are shorter than those of IF_5 (Table 5). To investigate the point further, a normal coordinate analysis of the fundamental frequencies of XeF_5^+ was undertaken, based on data for $[XeF_5^+][RuF_6^-]$ (which provides the optinum

combination of accurate geometry and sureness of assignment).

The valence force field for XeF_5^+ contains 20 force constants,[23] but only nine fundamentals are observed; the system is clearly underdetermined, and some assumptions must be made about the force field. Our approach initially involved the transfer of interaction constants from related molecules. A detailed treatment by Curtis[23] has given uncertainty limits for the force constants of IF_5 and $XeOF_4$; moreover, f_{rR} is usually assumed to be zero in C_{4v} systems with massive central atoms.[24] IF_6^+ was also considered since it has unusual vibrational properties ($\nu_3 > \nu_2 > \nu_1$); the most noticeable feature of its force field is $f_{rr} < 0$.[25] Good agreement with the experimental frequencies of XeF_5^+ was obtained in calculations using a simple 7 parameter force field:[26] $f_R = 4.3$, $f_r = 4.0$, $f_{rr'} = 0.1$ (mdyne Å^{-1}), $f_\beta = 2.1$, $f_\alpha = 0.75$, $f_{\beta\beta'} = 0.1$, $f_{\alpha\alpha} = 0.04$ (mdyne Å^{-1}). The values of the interaction force constants all lie within the limits suggested by Curtis for IF_5 and $XeOF_4$; the value of f_{rr} (i.e. zero) lies between those for IF_5 (0.06) and IF_6^+ (-0.06).

The simplicity of this force field may be deceptive. There are very short intramolecular F...F interactions in XeF_5^+ (e.g. $F_{ax}...F_{bas}$ = 2.32 Å); it would be surprising if these were not reflected in the force constants, and especially in the stretch-stretch interactions. Several solutions were tried with non-zero values for the interactions f_{rr}, f_{rR}, $f_{R\beta}$, $f_{r\alpha}$, and $f_{r\alpha'}$ (within the limits suggested by Curtis), yielding different values for the principal force constants and suggesting limits, viz. $f_R = 4.25 \pm 0.2$ and $f_r = 3.95 \pm 0.2$ mdyne Å^{-1} within which they probably lie. Comparison with other xenon fluorides shows that

these force constants are about right; correlations of bond lengths and stretching constants by the methods of Badger[27] and Herschbach-Laurie[28] give excellent straight lines (Figure 3). Moreover, the force constants listed in Table 5 show that the IF_5/XeF_5^+ anomaly is restricted to the axial bond; the smooth increase in the force constants of the basal bonds across the series SbF_5^{2-} - XeF_5^+ is similar to the increase in $\underline{f_r}$ found for SbF_6^-, TeF_6, and IF_6^+.[25] It may well be that repulsion between axial and basal fluorine atoms plays an important role in lengthening and weakening the axial bond in the XeF_5^+ cation.

(ii) $\underline{Xe_2F_{11}^+}$ Salts

The Raman frequencies of the solids $[Xe_2F_{11}^+][AuF_6^-]$, $[Xe_2F_{11}^+][PF_6^-]$, and $[Xe_2F_{11}^+][AsF_6^-]$ are listed in Table 6, together with frequencies for the cation in HF solution, derived from the spectra of the hexafluorophosphate and -arsenate salts; the spectra of $[Xe_2F_{11}^+][PF_6^-]$ are illustrated in Figure 2.

Anion lines are readily distinguished in the Raman spectra of these salts, since deviations from idealoctahedral behaviour are fewer than in the XeF_5^+ derivatives; however, ν_3 and ν_4 are observed, and some small splittings are also noted. After anion features are accounted for, a distinctive Raman pattern attributable to $Xe_2F_{11}^+$ is observed for the solids and for $Xe_2F_{11}^+$ in solution, strongly suggesting that the $Xe_2F_{11}^+$ ion everywhere resembles that defined crystallographically in $[Xe_2F_{11}^+][AuF_6^-]$. Distinct correspondences to the spectrum of XeF_5^+, evident in Figure 2, allow the facile interpretation of the $Xe_2F_{11}^+$ features in terms of two XeF_5^+ units linked by a bridging fluoride ion (Tables 6 and 7).

The stretching frequencies of $Xe_2F_{11}^+$ lie slightly lower than those of XeF_5^+, as might be expected since the overall charge *per* xenon atom is $+\frac{1}{2}$, the deformations, however, have about the same values. A Raman line at *ca.* 260 cm^{-1} is observed for all three salts, and for $Xe_2F_{11}^+$ in HF solution, where it is polarized; this line is apparently characteristic of $Xe_2F_{11}^+$, but its origin is not immediately clear. It lies at too high frequency for the symmetric stretching mode of the $F_5Xe^+...F^-...XeF_5^+$ bridging unit, since this assignment would imply a force constant of *ca.* 10 mdyne $Å^{-1}$ for the bridging bond; moreover, it has been shown that the vibration of an ion-pair generates only a very weak Raman line,[29] so that the relatively high intensity of 360 cm^{-1} feature is inconsistent with the vibration of an essentially ionic bridging unit. We believe that the line arises in coupling of the ν_3 deformations of the XeF_5^+ units *via* the symmetric stretch of the bridge; ν_3, which involves some motion of the xenon atom, and occurs at *ca.* 300 cm^{-1} in the free XeF_5^+ cation. Coupling *via* the bridge probably produces the splitting of the symmetric basal XeF_4 stretch observed for the solid $Xe_2F_{11}^+$ salts, and the great enhancement of the relative intensity of the axial XeF stretch (compared with the situation for XeF_5^+).

The Raman spectrum of $[Xe_2F_{11}^+][PF_6^-]$ in HF solution shows, in addition to $Xe_2F_{11}^+$ and PF_6^- features, a polarized line at 621 cm^{-1} attributable to XeF_5^+. The intensity of the XeF_5^+ line relative to $Xe_2F_{11}^+$ increases as the concentration of the solution decreases, suggesting the equilibrium

$$Xe_2F_{11}^+ + HF \rightleftharpoons 2XeF_5^+ + HF_2^-$$

in solution.

Xenon Hexafluoride

Before discussing the Raman spectra of xenon hexafluoride and their chemical consequences, it will be useful to review the colours of the compound in various phases. The vapour and liquid are yellow-green and the vapour is photosensitive, even to red light, decomposing to XeF_4;[14] the solid is white, except close to the melting point, when a yellow colour appears. Solutions in HF are yellow, but the colour decreases on dilution, and disappears on cooling.[30] Solutions in WF_6 are yellow-green, and the colour persists on dilution and on cooling.[31] It was mentioned above that solutions of XeF_5^+ and $Xe_2F_{11}^+$ in HF are colourless.

(i) Solid and Liquid

Gasner and Claassen[13] have reported the Raman spectra of solid and liquid xenon hexafluoride. We examined solid xenon hexafluoride during this study, obtaining spectra which tallied exactly with the earlier results. Our solid samples were either freshly sublimed or freshly solidified from the liquid, and it therefore seems certain that we were investigating Phase I, or one of the phases with which it interconverts thermally, containing only $[XeF_5^+F^-]_4$ tetramers. (Crystals of Phase IV, containing both tetramers and hexamers, are formed only by slow vapour transport at room temperature.[9]) The data for XeF_5^+ and $Xe_2F_{11}^+$ were used to assign the spectrum of solid xenon hexafluoride in terms of $[XeF_5^+F^-]_4$ tetramers (Table 7). The $[XeF_5^+F^-]_4$ frequencies are naturally lower, since the overall charge on the unit is zero. The intensity of the Raman line associated with the symmetric axial stretch of the XeF_5^+ units in the tetramer (at 656 cm^{-1}) is much more intense than the basal stretch (at 583 cm^{-1}), unlike XeF_5^+.

The Raman spectrum of liquid xenon hexafluoride at 54°C strongly resembles that of the solid, suggesting that the tetramer is the dominant species present; the enhanced intensity of some lines at 92°C will be discussed below.

(ii) Xenon Hexafluoride in WF_6

Spectra of solutions of xenon hexafluoride in WF_6 are listed in Table 8 and shown in Figure 4. The four Raman lines of the solvent obscure part of the spectrum, and a line at 554 cm^{-1}, assigned to XeF_4, was observed for some samples. Nevertheless, it is clear that, the $XeOF_4$ impurity apart, only two scattering Xe(VI) species are present in solution, and that the relative concentrations of these species change with the concentration of the solution. The changes in the spectrum, on dilution of the solution, parallel those seen on warming liquid xenon hexafluoride. (Table 8).

Strong polarized lines at 652 cm^{-1} and 585 cm^{-1} identify the $[XeF_5^+F^-]$ tetramer, and this is clearly the principal solute species in concentrated solution. The polarized Raman line at 621 cm^{-1} and the depolarized line at 508 cm^{-1} increase in intensity (relative to 652 cm^{-1}) in more dilute solution; their frequencies, relative intensities, and states of polarization correspond with the extra lines in hot liquid xenon hexafluoride, and, a little less closely, with the Raman spectrum of the vapour,[14] (Table 8) which contains only XeF_6 molecules.[32] We have little hesitation, therefore, in assigning these lines to a monomeric XeF_6 molecule. It is noteworthy that the thermodynamic properties of liquid xenon hexafluoride (especially the anomalously high heat capacity) have

similarly been explained in terms of an equilibrium involving a tetramer and monomer.[33] The photolysis of XeF_6 molecules in solution would explain the observation of XeF_4, and the intensity of the XeF_4 peak increases the longer the sample was exposed to the laser beam.

There is no evidence for discrete ionic fluoroxenon species in WF_6 solution. In addition to the lack of spectroscopic correspondence with the XeF_5^+ and $Xe_2F_{11}^+$ cations, the following pieces of evidence may be cited to support this view

(i) Compounds such as $XeF_5^+BF_4^-$ are insoluble in WF_6.

(ii) Removal of solvent from solutions of XeF_6 in WF_6 by pumping at low temperature leaves pure xenon hexafluoride.

(iii) A ^{19}F n.m.r. study of xenon hexafluoride in WF_6[34] shows no exchange between xenon hexafluoride, solvent, and the $XeOF_4$ impurity.

Our results add little to the question of the structure of the xenon hexafluoride molecule. The polarized Raman line at 621 cm^{-1} could be assigned to the $\nu_1(\underline{a}_{1g})$ stretch of an octahedral molecule, and the depolarized line at 508 cm^{-1} to $\nu_2(\underline{e}_g)$; the intensity pattern (ν_2 is comparable with ν_1) is very reminiscent of the Raman spectra of some isoelectronic molecules which are octahedral, _viz._ the hexahalogenotellurates(IV).[35] Octahedral symmetry, however, cannot be reconciled with the complicated infrared spectrum of XeF_6 vapor,[36] at least in the approximation of a simple harmonic corce field. Pitzer and Bernstein have in any case provided persuasive evidence[37] for XeF_6 monomer being substantially distorted in the T_{1u} bending mode from octahedral symmetry. This is in essential agreement with the bonding model proposed by Bartell and Gavin.[38]

(iii) Xenon Hexafluoride in HF

Hyman and Quarterman showed that solutions of xenon hexafluoride in HF conduct electricity, but that the compound is not fully ionized; a Raman line at 620 cm^{-1} was observed for a solution of unspecified concentration, but the identity of the conducting species was not ascertained.[30] ^{19}F n.m.r. studies show that xenon hexafluoride exchanges with HF.[39] We examined the spectra of solutions of xenon hexafluoride in HF as a function of concentration; typical results, together with assignments of the lines, are given in Table 9, and illustrated in Figure 5.

The spectra change with the concentration of the solution. In concentrated solution the pattern is reminiscent of $[XeF_5^+F^-]_4$ and this must be the major species present; at intermediate concentrations the main spectroscopic features closely resemble those of $Xe_2F_{11}^+$ in HF; and in dilute solution the Raman spectrum is dominated by lines due to XeF_5^+. No Raman lines due to the anion HF_2^- or its solvates are observed, but this is common for HF solutions. Xenon hexafluoride clearly behaves as a base in anhydrous hydrogen fluoride, and the principal equilibria may be written:

$$[XeF_5^+F^-]_4 + 2\ HF \rightleftharpoons 2\ Xe_2F_{11}^+ + (HF)_xF^-$$

$$Xe_2F_{11}^+ + HF \rightleftharpoons 2\ XeF_5^+ + (HF)_xF^-$$

The spectra also show a weak depolarized line at ca. 510 cm^{-1}, which is assigned to molecular XeF_6; the corresponding polarized line at ca. 620 cm^{-1} is obscured by cation stretching features. The presence of some monomer accounts for the color of the HF solutions, and the temperature

dependence of the tetramer-monomer equilibrium accounts for the disappearance of the color on cooling. Ionization is the major process, however.

GENERAL DISCUSSION

Except for the monomolecular XeF_6 species which appears to be much the same in solution in WF_6 and HF as it is in the gas phase, all of the other neutral and cationic species in solution can be described approximately as XeF_5^+ or as clusters of this ion with F^-. The existence of the $(XeF_5^+F^-)_4$ tetramer in equilibrium with XeF_6 monomer in the non-ionizing solvent WF_6, demonstrates the ease with which the monomer ionizes.

The ideal XeF_5^+ ion has C_{4v} symmetry and it is not far from this symmetry in the XeF_5MF_6 salts[5,6,9]; but even in the $Xe_2F_{11}^+$ salts[8] and in crystalline[9] XeF_6 the departure from the idealized symmetry is not great. The vibrational data is in harmony with this view. Evidently one XeF bond (the axial) is always significantly stronger than the other four. All structures support the assumption that the non-bonding-xenon-valence-electron pair is situated on the four-fold axis trans to the short (axial) bond. When XeF_5^+ clusters with F^- either in making species such as $Xe_2F_{11}^+$ or $(XeF_5^+F^-)_4$, the bridging F^- avoids the four-fold axis, where the non-bonding-Xe-electron pair is presumed to be situated, and lies above a face of the pseudo-octahedron representing the XeF_5^+. Our vibrational data are in accord with the simple ionic assembly model (allowing for appropriate polarization of the component XeF_5^+ and F^-) for $Xe_2F_{11}^+$ and the other clusters.

The relationship of XeF_5^+ to its isoelectronic relatives IF_5, TeF_5^- and SbF_5^{2-}, which is brought out in Table 5, is remarkable for the constancy of the angle F_{ax}-E-F_{bas}. It is indicative of a constant

hybridization of the central atom (E) orbitals across the series. Moreover the axial bond ($E-F_{ax}$) is much stronger relative to the basal bond ($E-F_{bas}$) in SbF_5^{2-} and the two bonds approach equality as the nuclear charge (Z) of E increases. This is consistent with the representation of $E-F_{bas}$ as three-center-four-electron bonds, in consequence of which the F_{bas} ligands bear considerable negative charge.[40] The negatively charged F_{bas} will experience increased attraction to E as the nuclear charge of that atom increases and F_{eq} which is to be viewed as electron-pair bonded to E, will be closer to charge neutrality than F_{bas} and its attraction to E will in consequence be less dependent upon Z of E.

The vibrational data show that the monomer of XeF_6 in solution is essentially the same as in the gas phase. Electron diffraction data for the latter have been interpreted by Pitzer and Bernstein[37] in terms of a static $\underline{C_{3v}}$ model with XeF = 1.850 and 1.941 Å (each with a multiplicity of three) and indicate that the non-bonding-Xe-electron pair has steric activity and is situated on the three fold axis on the long-bonded side of the molecule. This steric activity of the non-bonding 'pair' need not imply that d or other outer Xe orbitals are involved in the bonding as the simple-valence-electron-pair-repulsion model implies.[41] Indeed the molecular orbital approach of Bartell and Gavin[38] permits the XeF_6 behavior to be rationalized on the basis of a near degeneracy of the filled A_{1g}^* orbital, of octahedrally symmetric XeF_6, with the empty T_{1u}^* set of orbitals. This provides for a second-order Jahn-Teller distortion. This molecular orbital description leaves the question of the degree of involvement of the outer d orbitals unanswered. Symmetry and the ligand field

are such that two of these d orbitals are probably involved in bonding- at least slightly. It seems that in $TeCl_6^{2-}$ and related species,[35] the A_{1g}^* and T_{1u}^* orbitals in octahedral symmetry are not sufficiently close in energy for this dynamic Jahn-Teller effect to appear. Perhaps this is a consequence of the large size of the Cl ligand compared with F. The ligand charge in the chloride is neither as concentrated nor as close to the Xe $5s^2$ electrons. The promotion of the Xe $5s^2$ electrons to a directional orbital requires energy. In XeF_6 monomer this is presumably provided by enhanced bonding, which derives from the increase in the effective positive charge at the Xe(VI) atom, as the non-bonding 'pair' is promoted from $5s^2$ to an orbital directed away from the ligands.

The greater ease of ionization of XeF_6 compared with either XeF_4 or XeF_2 calls for comment. It is evident that XeF_6 with a sterically active non-bonding electron pair, plus the six F ligands, has a more crowded ligand situation than can occur in either XeF_4 or XeF_2 and it must be supposed that this more than offsets the greater charge at the Xe atom. Certainly the non-bonding electron-pair in XeF_6 no longer approximates to $5s^2$. It is quite probable, however, that one of the Xe non-bonding electron pairs in XeF_4 and in XeF_2 can be approximately so described. If so the conversion of XeF_2 to XeF_4 simply removes a Xe $5p^2$ pair of electrons from a non-bonding role[40] whereas the conversion of XeF_4 to XeF_6 not only does the same again but brings the remaining Xe valence 'pair' into the ligand repulsion sphere for the first time - thus compounding the repulsive interactions.

ACKNOWLEDGEMENTS

We are indebted to Dr. J. Scherer, U.S.D.A. Western Regional Laboratories, Albany, California, for access to Raman facilities. C.J.A. thanks the Commonwealth Fund for a Harkness Fellowship (1971-73). The work was otherwise supported by the U. S. Atomic Energy Commission and was recently by the Division of Basic Energy Sciences, U. S. Department of Energy.

References

1. Based on a paper presented at the Autumn Meeting of the Chemical Society, Dalton Division, Norwich, September 1973.
2. Present address: Port Sunlight Laboratory, Unilever Ltd., Port Sunlight, Merseyside L62 4XN, England.
3. N. Bartlett and F. O. Sladky, J. Amer. Chem. Soc., 1968, 90, 5316.
4. J. Berkowitz, W. A. Chupka, P. M. Guyon, J. H. Holloway, and R. Spohr, J. Phys. Chem., 1971, 75, 146.
5. N. Bartlett, M. Gennis, D. D. Gibler, B. K. Morrell, and A. Zalkin, Inorg. Chem., 1973, 12, 1717.
6. N. Bartlett, B. G. De Boer, F. J. Hollander, F. O. Sladky, D. H. Templeton, and A. Zalkin, Inorg. Chem., 1974, 13, 780.
7. K. Leary, D. H. Templeton, A. Zalkin, and N. Bartlett, Inorg. Chem., 1973, 12, 1726.
8. K. Leary, A. Zalkin, and N. Bartlett, J.C.S. Chem. Commun., 1973, 132, and Inorg. Chem., 1974, 13, 775.
9. R. D. Burbank and G. R. Jones, Science, 1971, 171, 485; J. Amer. Chem. Soc., 1974, 96, 43.

9a. K. O. Christe, E. C. Curtis, and R. D. Wilson, J. Inorg. Chem., Supplement 1976, 159.

10. N. Bartlett and M. Wechsberg, Z. anorg. allg. Chemie, 1971, 385, 5.
11. D. D. Desmarteau and M. Eisenberg, Inorg. Chem., 1972, 11, 2641.
12. B. Frlec, M. Bohinc, P. Charpin, and M. Drifford, J. Inorg. Nuclear Chem., 1972, 34, 2938.
13. E. L. Gasner and H. H. Claassen, Inorg. Chem., 1967, 5, 1937.
14. H. H. Claassen, G. L. Goodman, and H. Kim, J. Chem. Phys., 1973, 55, 5042.

References (Contd.)

15. J. G. Malm, F. Schreiner and D. W. Osborne, Inorg. Nuclear Chem. Letters, 1965, 1, 97.

16. H. Selig, Science, 1964, 144, 537.

17. N. Bartlett, S. P. Beaton, and N. K. Jha, Abstracts 148th Meeting, Amer. Chem. Soc., 1964, K3.

18. K. E. Pullen and G. H. Cady, Inorg. Chem., 1967, 6, 2267.

19. N. Bartlett, F. Einstein, D. F. Stewart, and J. Trotter, J. Chem. Soc. (A), 1967, 1190.

20. K. Leary and N. Bartlett, J.C.S. Chem. Commun., 1972, 903.

21. M. Brownstein and J. Shamir, Applied Spectroscopy, 1972, 26, 77.

22. H. Selig and H. Holzman, Israel J. Chem., 1969, 7, 417.

23. E. C. Curtis, Spectrochimica Acta, 1971, 27A, 1989.

24. K. O. Christe, E. C. Curtis, C. J. Schack, and D. Pilipovich, Inorg. Chem., 1972, 11, 1679.

25. K. O. Christe and W. Sawoduy, Inorg. Chem., 1967, 6, 1783.

26. The geometry of XeF_5^+ in $[XeF_5^+RuF_6^-]$ is summarized in Table 3; $\angle F_{bas}\text{-}Xe\text{-}F_{ax}(\alpha) = 90°$. Frequencies were calculated from the geometry and an assumed force field using the program CRDAN, written by Dr. V. Bondebey, and made available by Prof. G. Pimentel. Primed interaction constants refer to opposite coordinates, and unprimed to adjacent coordinates.

27. R. M. Badger, J. Chem. Phys., 1934, 2, 128.

28. D. R. Herschbach and V. W. Laurie, J. Chem. Phys., 1961, 35, 458.

29. J. H. B. George, J. A. Rolfe, and L. A. Woodward, Trans. Faraday Soc., 1953, 49, 375.

30. H. H. Hyman and L. A. Quarterman, in "Noble Gas Compounds", ed. H. H. Hyman, Chicago, 1963, p. 275.

References (Contd.)

31. Similar colors are observed for BrF_5 and IF_5 solutions of xenon hexafluoride.

32. Mass spectroscopic investigation shows less than 1 part in 10^6 polymer; W. E. Falconer personal communication.

33. F. Schreiner, D. W. Osborne, J. G. Malm, and G. N. McDonald, J. Chem. Phys., 1969, 51, 4838.

34. N. Bartlett, S. P. Beaton, E. J. Wells, and L. W. Reeves, unpublished observation, University of British Columbia, 1965.

35. C. J. Adams and A. J. Downs, J.C.S. Chem. Commun., 1970, 1699.

36. H. Kim, H. H. Claassen, and E. Pearson, Inorg. Chem., 1968, 7, 616.

37. K. S. Pitzer, and L. S. Bernstein, J. Chem. Phys., 1975, 63, 3849.

38. L. S. Bartell, and R. M. Gavin, Jr., J. Chem. Phys., 1968, 48, 2466.

39. T. H. Brown, E. B. Whipple, and P. H. Verdier, in "Noble Gas Compounds", ed. H. H. Hyman, Chicago, 1963, 263.

40. N. Bartlett, and F. O. Sladky, "The Chemistry of Krypton, Xenon and Radon," in "Comprehensive Inorganic Chemistry," J. C. Bailor, et al. ed., Pergamon Press, Oxford and New York, 1973, Vol. I, pp. 213-330.

41. S.-E. Karlsson, K. Siegbahn and Neil Bartlett, UCRL Report 18502, Sept. 1969 and T. X. Carroll, R. W. Shaw, Jr., T. D. Thomas, C. Kindle, and N. Bartlett, J. Amer. Chem. Soc., 1974, 96, 1989.

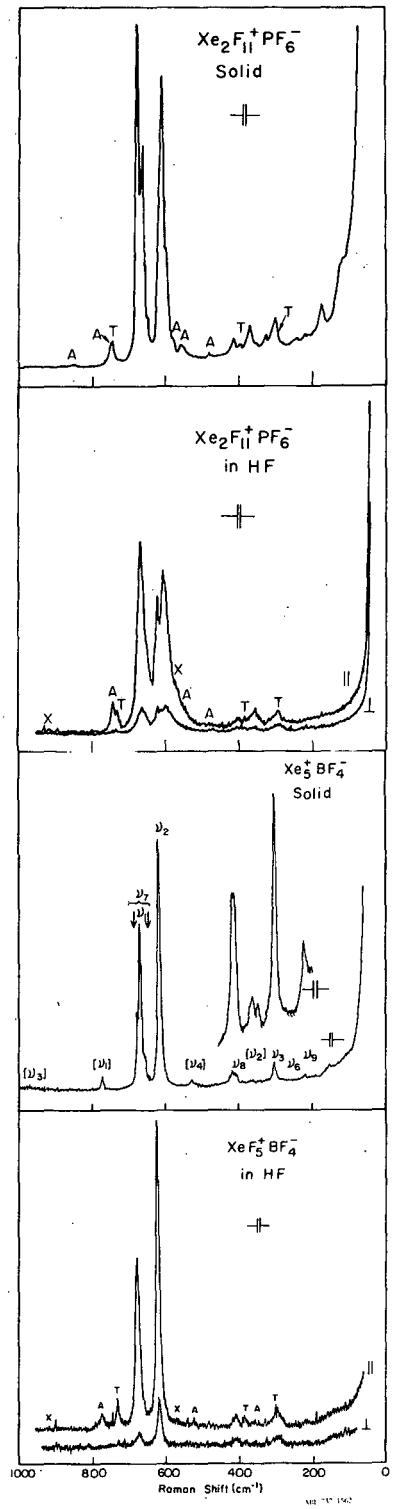
$Xe_2F_{11}^+PF_6^-$
Solid
$Xe_2F_{11}^+PF_6^-$
in HF
$Xe_5^+BF_4^-$
Solid
$XeF_5^+BF_4^-$
in HF
Raman Shift (cm⁻¹)
1000
800
600
400
200
0

Fig. 1

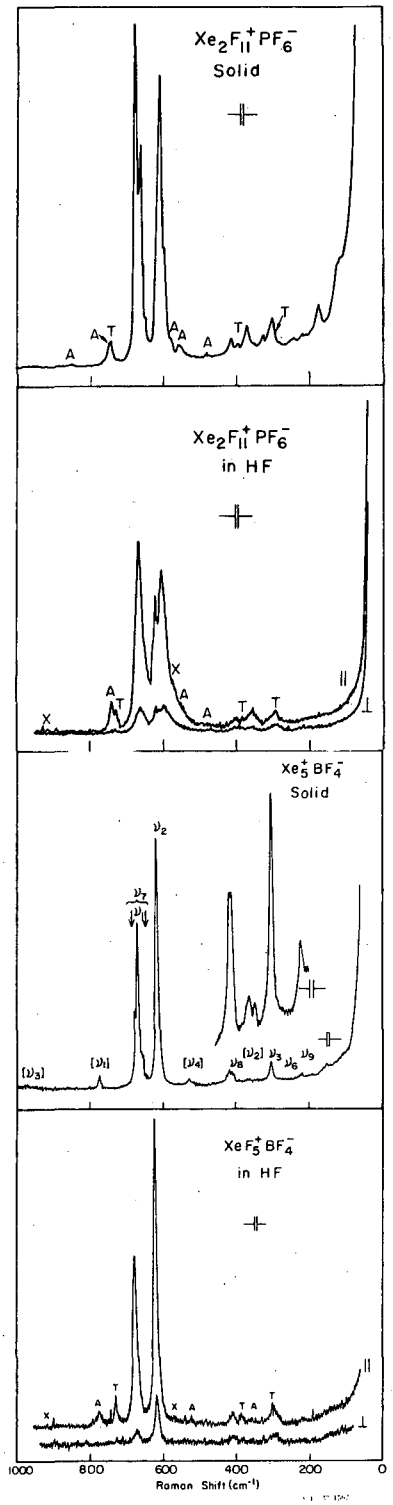
$Xe_2F_{11}^+PF_6^-$
Solid
$Xe_2F_{11}^+PF_6^-$
in HF
$Xe_5^+BF_4^-$
Solid
$XeF_5^+BF_4^-$
in HF
1000
800
600
400
200
0
Raman Shift (cm⁻¹)

Fig. 2

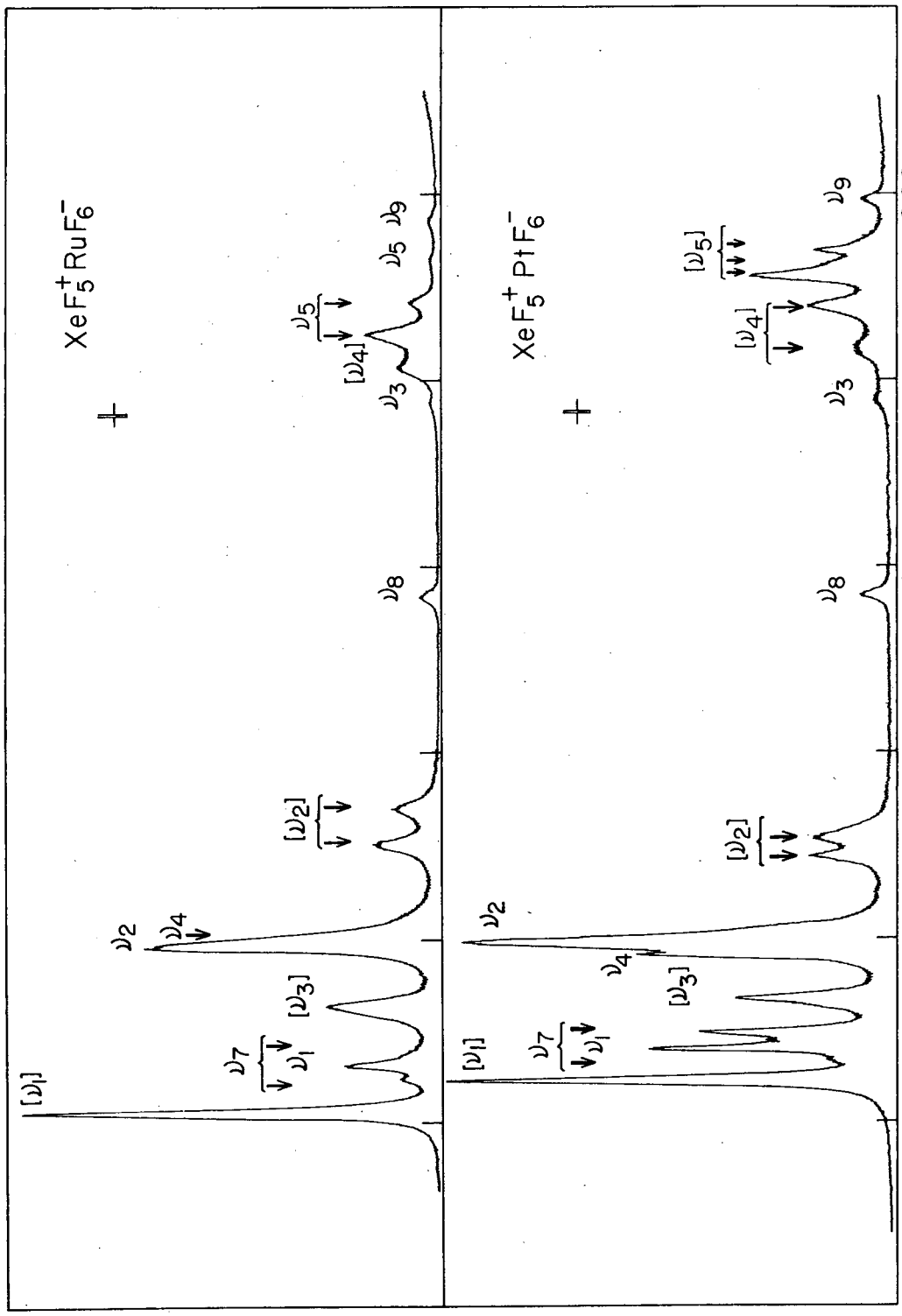

XBL 737-6405

Fig. 5

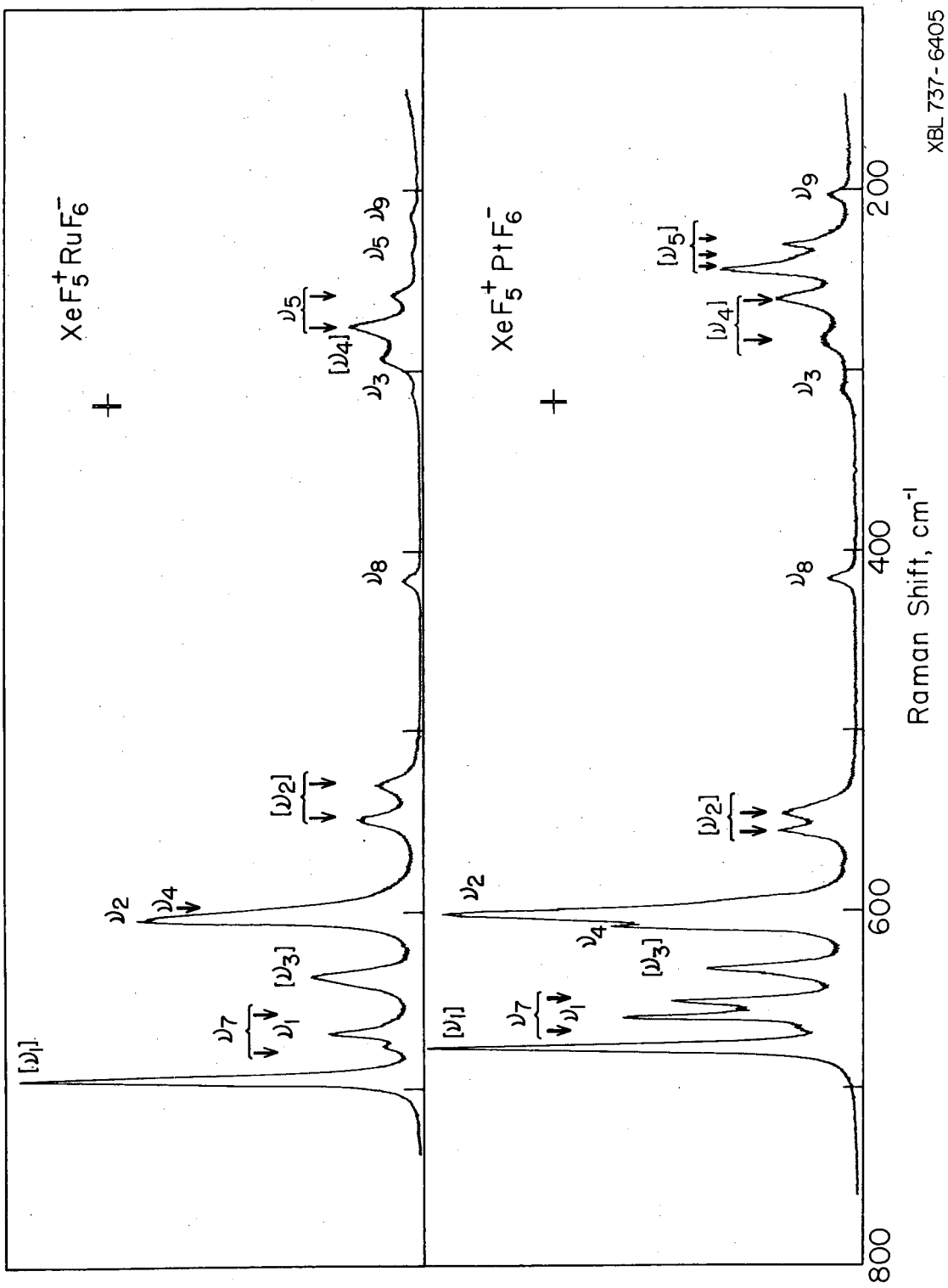

XBL 737-6405

Fig. 4

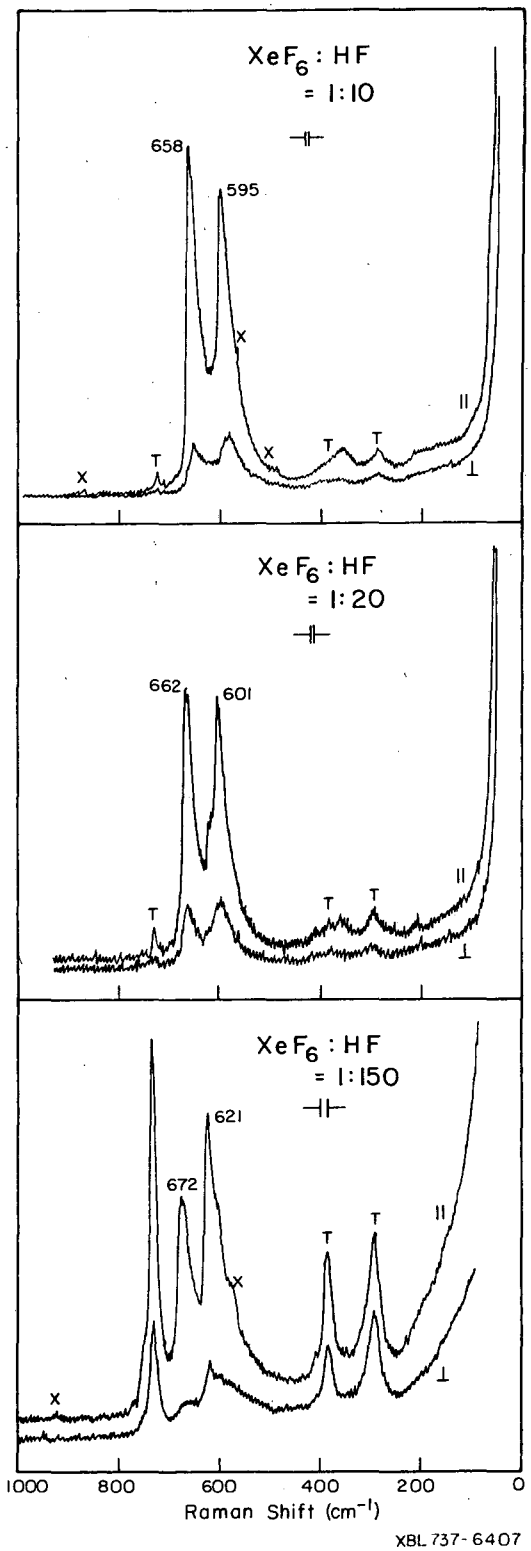
XeF6 : HF
= 1:10
658
595
X
T
T
T
II
⊥
XeF6 : HF
= 1:20
662
601
T
T
T
II
⊥
XeF6 : HF
= 1:150
621
672
T
T
T
II
⊥
1000
800
600
400
200
0
Raman Shift (cm-1)
XBL 737-6407

Fig. 5

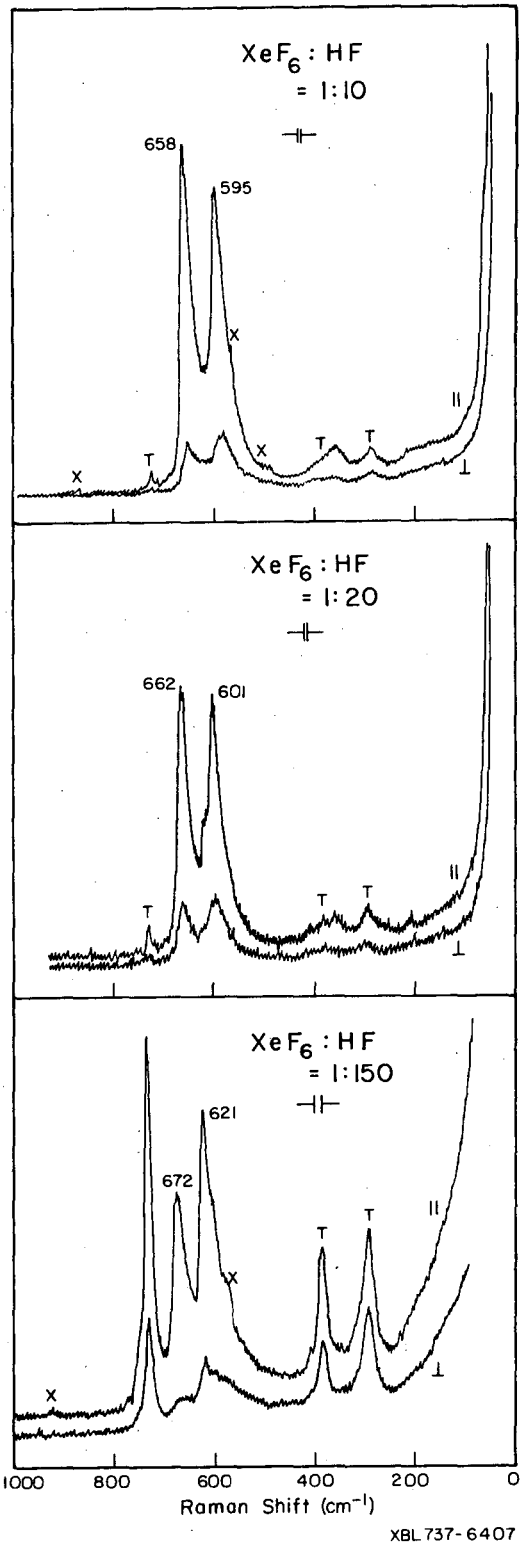
XeF6 : HF
= 1:10
658
595
X
T
X
T
T
II
⊥
XeF6 : HF
= 1:20
662
601
T
T
T
II
⊥
XeF6 : HF
= 1:150
621
672
X
T
T
II
⊥
X
1000
800
600
400
200
0
Raman Shift (cm⁻¹)
XBL737-6407

Fig. 6

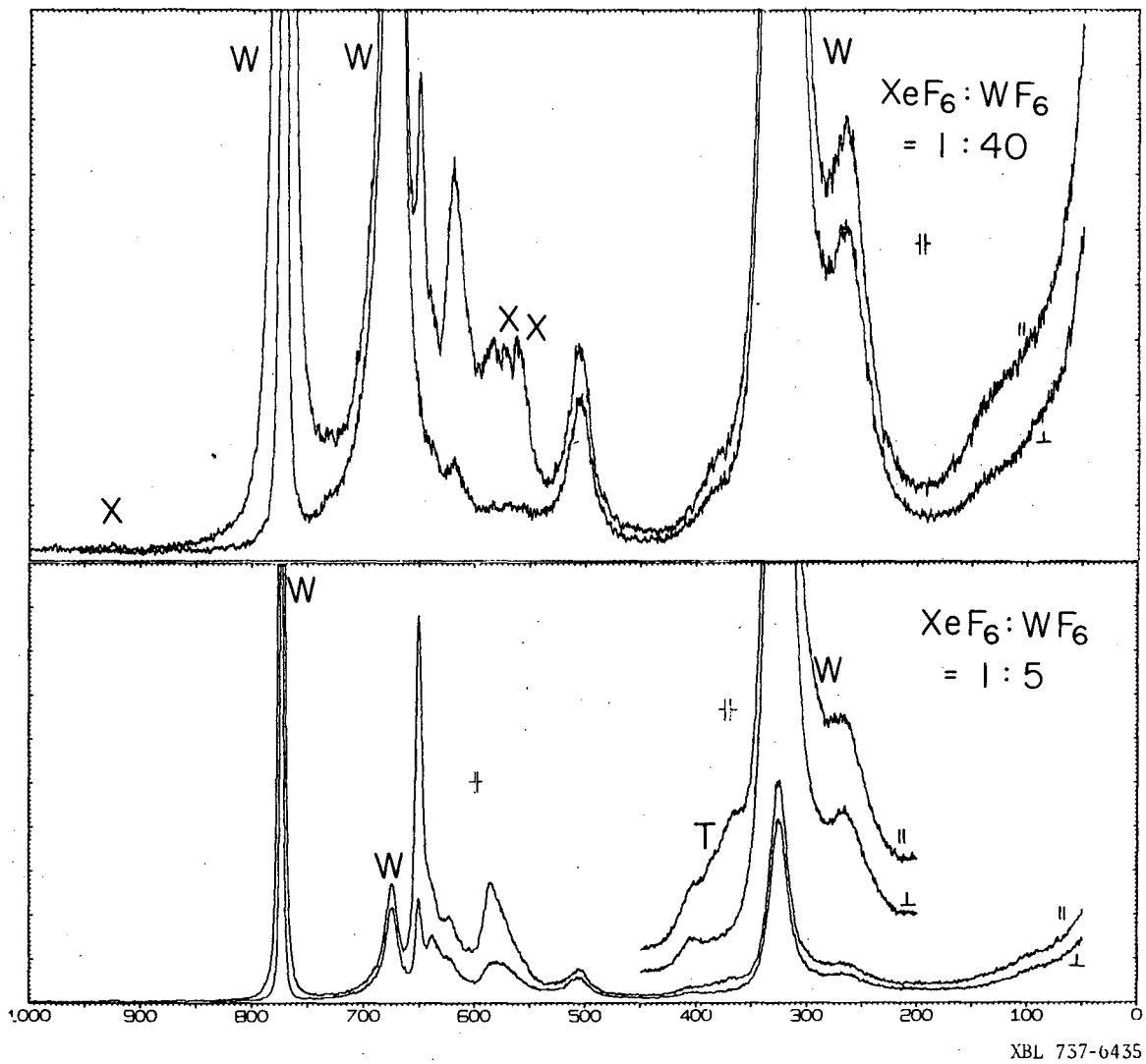
W
W
W
XeF6 : WF6
= 1 : 40
X
X X
W
W
XeF6 : WF6
= 1 : 5
W
T
1,000
900
800
700
600
500
400
300
200
100
0
XBL 737-6435

Fig. 7

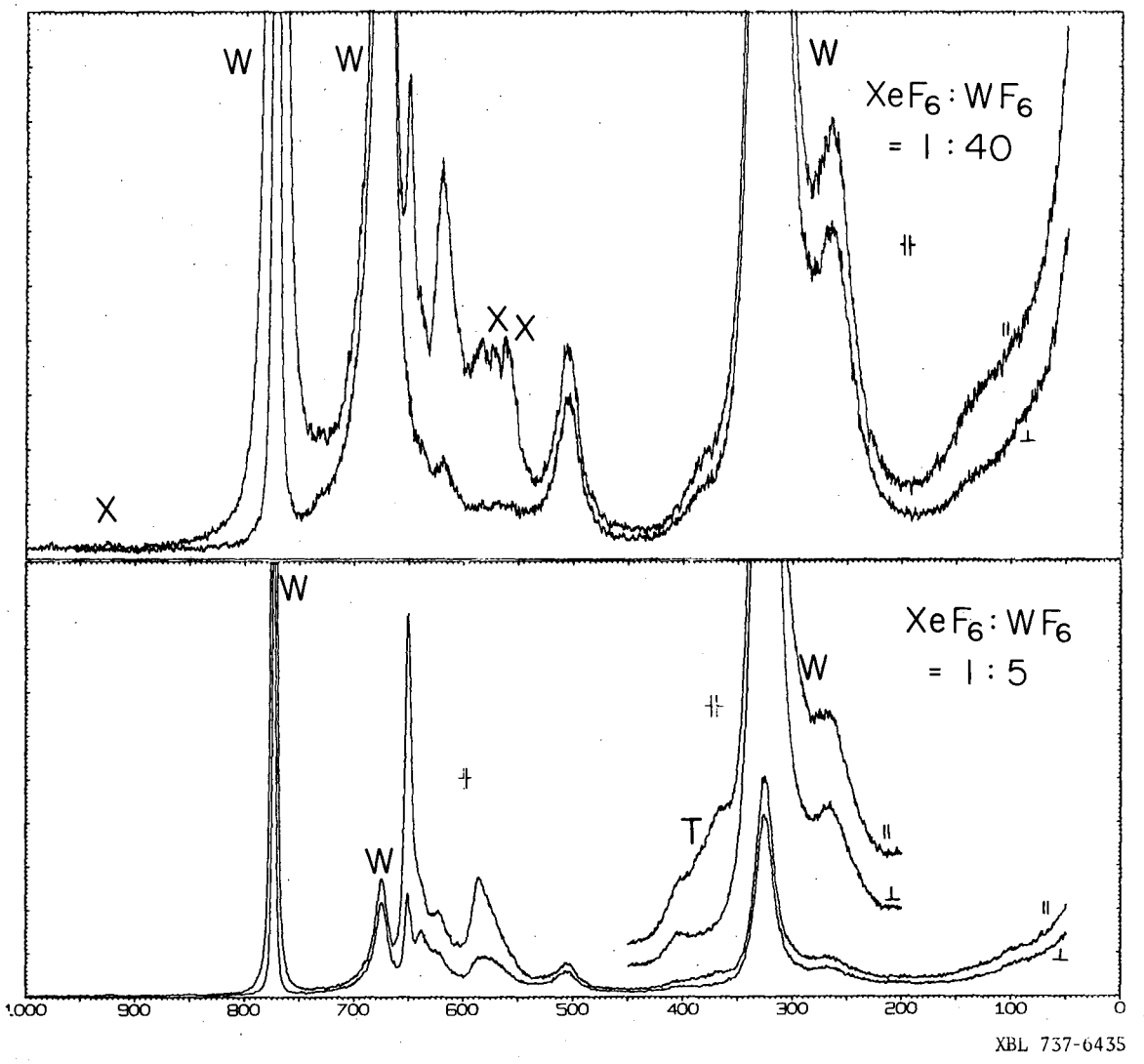
W
W
X
X
X
W
XeF6 : WF6
= 1 : 40
W
W
W
T
XeF6 : WF6
= 1 : 5
1,000
900
800
700
600
500
400
300
200
100
0
XBL 737-6435

Fig. 8

TABLE 1

Raman and Infrared Spectra of $[XeF_5^+][BF_4^-]$

$[XeF_5^+][BF_4^-]$						Assignment	
Solid (25°C) Raman		Solid (-196°) Infrared		HF Solution (0.5 M) Raman			
cm^{-1}	Rel.Int.	cm^{-1}	Rel.Int.	cm^{-1}	Pol. Rel.Int.	XeF_5^+	BF_4^-(b)
993,b 962	2 2	~1000	s, vb	~1050,b	dp 0+		$\nu_3(t_2)$, $2\nu_4$
772	6	769	vw	776	p 3		$\nu_1(a_1)$
667	65	672	ms	676	p 50	$\nu_1(a_1)$	
673 654	19 5	650	s	[676]		$\nu_7(e)$	
614	100			621	p 100	$\nu_2(a_1)$ $\nu_4(b_1)$	
524	3	536 523	w w	522	dp 3		$\nu_4(t_2)$
416 409	4 4			408	dp 7	$\nu_8(e)$	
360 344	0+ 0+			358	dp 3		$\nu_2(e)$
302	7			301	p? 7	$\nu_3(a_1)$	
263	0+			255,b	dp 0+	$\nu_6(b_2)$	
219	1			216	dp 2	$\nu_9(e)$	
152	3					Lattice Vibration	

[a] Excited at 4880 Å.

[b] Frequencies for solid KBF_4. Raman: 773 vs. (ν_1), 536, 529 mw (ν_4), 358 m (ν_2); M. Azeem, M. Brownstein, and R. J. Gillespie, Canad. J. Chem., 1969, 47, 4159. Infrared: 1078, 1063, 1036 vs. (ν_4), 772 vw (ν_1) 536, 525 m (ν_4); N. N. Greenwood, J. Chem. Soc., 1959, 3811.

TABLE 2

Raman Spectra of XeF_5^+ Salts with Hexafluoroanions

	$[XeF_5^+][AsF_6^-]$					$[XeF_5^+][AuF_6^-]$		$[XeF_5^+]_2[PdF_6^{2-}]$(a)		$[XeF_5^+RuF_6^-]$		$[XeF_5^+][PtF_6^-]$		Assignment
Phase	Solution in HF(0.5M)			Solid		Solid		Solid		Solid		Solid		
Exciting line	4880Å			4880Å		4880Å		6328Å		4880Å		6471Å		
	cm^{-1}	pol.	Rel.Int.	cm^{-1}	Rel.Int.	cm^{-1}	Rel.Int.	cm^{-1}	Rel.Int.	cm^{-1}	Rel.Int.	cm^{-1}	Rel.Int.	
Cation lines														XeF_5^+
	677	p	60	671	29	681	23	653	100	670	22	661	54	$\nu_1(a_1)$
	[677]			664,sh	5	690	24	676	3	677	9	666	3	$\nu_7(e)$
				661	30	669	5	660,sh	5	664,sh	1	652	43	
	625	p	100	629	100	581	94	590	71	606	68	603	97	$\nu_2(a_1)$
	[625]			623,sh	~5	577	72	606	20	~600,sh	~10	610	56	$\nu_4(b_1)$
	410	dp	4	412	6	411	2	425	3	416	4	411	8	$\nu_8(e)$
				407	6	396	4	396	3					
	302	p?	3	296	15	303,sh	~3	309	10	312	2	311	3	$\nu_3(a_1)$
	255,b	dp	0+	255	1	251	0+							$\nu_6(b_2)$
				240	0+			230,b	4	236	1			$\nu_5(b_1)$
	216	dp	1	214	4	208	11	[230]		215	2	203	5	$\nu_a(e)$
Anion lines (b)														MF_6^{n-}(b)
				738	22	650	9	634	4	642,sh	3	637,sh	5	$\nu_3(t_{1u})$
				723	10	641	28	624	2	638	25	633	34	
				710	2	628	22	616	8					
						623,sh	~10							
	688,sh	p	~20	687	25	591	100	558	67	696	100	677	100	$\nu_1(a_{1g})$
	550,b	dp	4	550	7	543	0+	535	92	549	15	556	19	$\nu_2(e_g)$
				543	12	534	0+			530	11	546	17	
				397	6	296	5	295,b	7	293,b	10	284,b	7	$\nu_4(t_{1u})$
				393	12	283	1			280,sh	1	261		
				391	14	273	2							
				381	5									
				373	9	230	27	269	6	275	17	244	30	
	375	dp	~6	363	6	226	26	245	10	258	6	238,sh	~5	$\nu_5(t_{2g})$
				347	3	220,sh	2					231	16	
				343	3									
Lattice vibrations														
				~130,b	2					~140,b	1	~110,b	1	
										104,b	2	74	7	
										68	3			

(a) Spectrum made available by K. Leary.

(b) Anion frequencies: $CsAsF_6$; ν_1 685, ν_2 576, ν_3 699, ν_4 392, ν_5 372; G. M. Begun and A. C. Rutenberg, Inorg. Chem., 1967, 6, 2232.

$CsAuF_6$: ν_1 595, ν_2 530, ν_3 640, ν_5 224; Reference 20. $CsRuF_6$: ν_1 656, ν_2 581, ν_3 640, ν_5 269.

$[NO^+][PtF_6^-]$ ν_1 647, ν_2 590,572; ν_3 630; ν_5 249,236; F. O. Sladky, P. A. Bulliner, and N. Bartlett, J. Chem. Soc. (A), 1969, 2179.

$[NO^+]_2[PdF_6^{2-}]$; ν_1 573, ν_2 554, ν_3 610, ν_5 243, K. Leary and N. Bartlett, unpublished observations.

Table 3

Crystallographic Data for XeF_5^+ Salts

Compound	Crystal System	Space Group	Z	Site Symmetry		XeF_5^+ Bond lengths (Å)		F_{ax}-Se-F_{bas}	Reference
				Xe	M	R(ax)	r(bas)	3	
$[XeF_5^+][RuF_6^-]$	Orthorhombic	Pnma	4	m	m	1.79(1)	1.85(1)	79.0(6)	5
$[XeF_5^+][PtF_6^-]$	Orthorhombic	Pnmb	4	m	m	1.81(8)	1.88(8)	79.5(40)	19
$[XeF_5^+][AuF_6^-]$[b]	Monoclinic	$P2_1/c$	4	1	1	---	---	---	This work
$[XeF_5^+][AsF_6^-]$	Monoclinic	$P2_1/c$	4	1	1	1.76(2)	1.82(3)	80.4(15)	6
$[XeF_5^+][BF_4^-]$[a]	Orthorhombic	---	8	<222	<222	---	---	---	This work
$[XeF_5^+]_2[PdF_6^{2-}]$	Orthromhombic	$Pca2_1$	4	1	1	1.81(1)	1.84(1)	79.2(4)	7

a. $\underline{XeF_5^+BF_4^-}$ Orthorhombic: unknown space group, a = 8.41(2) Å, b = 8.60(2) Å, c = 17.47(4) Å, $\underline{V}$ = 1263.5, Z = 8.

b. $\underline{XeF_5^+AuF_6^-}$ Monoclinic, $P2_1/c$, a = 5.88(2), b = 16.54(4), c = 8.12(2), $\underline{V}$ = 791, $\underline{Z}$ = 4.

Table 4

Fundamental Frequencies of Some Square-Pyramidal Molecules

SbF_5^{2-}	TeF_5^-	IF_5 [c]	XeF_5^+ [d]	$XeOF_4$ [e]	Assignment in C_{4v} Symmetry		
					Class	Fundamental	Description
557	638	710	670	926.3	a_1	ν_1	ν MF(MO
427	524	616	606	576.9		ν_2	ν_s MF_4
278	281	318	312	285.9		ν_3	δ_s MF_4 (Umbralla)
388	494	604	600	543	b_1	ν_4	ν_{as} MF_4
			236	[214]		ν_5	δ_{as} MF_4 (out-of-plane)
220	240	276	[263]	225	b_2	ν_6	δ_s MF_4 (in-plane)
377	495	631	677	604	e	ν_7	ν_{deg} MF_4
359			644				
305	341	372	416	362		ν_8	δ $F_4MF(0)$
142	166	200	215	161		ν_9	δ_{as} MF_4 (in-plane)

[a] Solid K_2SbF_5; L. E. Alexander and I. R. Beattie, J. Chem. Soc (A), 1971, 3091.

[b] TeF_5^- in MeCN; data from C. J. Adams and A. J. Downs, ibid., 1971, 1534.

[c] Gaseous IF_5; Ref. 22.

[d] Solid $[XeF_5^+][RuF_6^-]$; ν_6 from $[XeF_5^+][BF_4^-]$; this work.

[e] Gaseous $XeOF_4$; P. Tsao, C. C. Cobb, and H. H. Claassen, J. Chem. Phys., 1971, 54, 5247.

Table 5

Dimensions and Force Constants for Some MX_5 Molecules

	SbF_5^{2-}	TeF_5^-	IF_5	XeF_5^+
M-F_{ax}(R),Å	1.916(4)[a]	1.862(4)[b]	1.844(25)[c]	1.793(8)[d]
M-F_{bas}(r),Å	2.073(3)	1.952(4)	1.869(s)	1.845(9)
$\angle F_{ax}$-M-F_{bas}(β)°	79.4(1)	78.8(2)	81.9(1)	79.0(17)
f_R, mdyne Å^{-1}	2.92[e]	3.56[f]	4.84[g]	4.5 ± 0.2[h]
f_r, mdyne Å^{-1}	1.67	2.27	3.64	3.95 ± 0.2

[a] K_2SbF_5; R. R. Ryan and D. T. Cromer, Inorg. Chem., 1972, 11, 2322.

[b] $KTeF_5$; S. H. Maskin, R. R. Ryan, and L. B. Asprey, ibid., 1970, 9, 2100.

[c] Gaseous IF_5; A. G. Robiette, R. H. Bradley, and P. N. Brier, J. C. S. Chem. Commun., 1971, 1567.

[d] $[XeF_5^+][RuF_6^-]$; Ref. 5.

[e] C. J. Adams and A. J. Downs, J. Chem. Soc. (A), 1971, 1534.

[f] Ref. 24.

[g] Ref. 23.

[h] This work.

TABLE 6

Raman Spectra of some $Xe_2F_{11}^+$ Salts

Compound	$[Xe_2F_{11}^+][PF_6^-]$		$[Xe_2F_{11}^+][AsF_6^-]$		$[Xe_2F_{11}^+][AuF_6^-]$		$[Xe_2F_{11}^+][MF_6^-]$(a)			Assignment
Phase	Solid		Solid		Solid		in HF solution			
Exciting line	4880Å		4880Å		6471Å		4880Å			
	cm^{-1}	Rel.Int.	cm^{-1}	Rel. Int.	cm^{-1}	Rel.Int.	cm^{-1}	pol.	Rel.Int.	
Cation lines										$Xe_2F_{11}^+$
	666	100	663	100	662	63	667,b	p	100	ν XeF_{ax}
	657 651 640	40 58 3	655,sh 644	44	640	2				ν_{deg} XeF_4
	604 598	46 70	602 594	36 60	601 592	48 72	605,b	p	85	ν_s XeF_4
	587	29	583	20	(c)		~590,b,sh	dp	~10	ν_{as} XeF_4
	402,b	4	408	2	400,b	1	410,b	dp	5	δ F_4XeF
	360	6	358	6	357,b	2	360,b	p	7	δ_s XeF_4
			298,sh	~1	295,sh	~1	302	p?	6	
	299	4	290	5	288	3				δ_s XeF_4(in-plane)
	230,b	0+	232	0+						$\delta_{as}XeF_4$(out-of-plane)
	207	0+	206	2	202	2	214,b	dp	0+	$\delta_{as}MF_4$(in-plane)
Anion lines										MF_6^- (b)
	848	0+	719	11	630	2				$\nu_3(t_{1u})$
	740	6	[663]		588	100				$\nu_1(a_1)(a_{1g})$
	570	4	564 551	8 4						$\nu_2(e_g)$
	547,b 540	3 2	390	5						$\nu_4(t_{1u})$
	470	1+	367	6	223	25				$\nu_5(t_{2g})$
	314	2	247	0+						$\nu_6(t_{2u})$
Lattice vibrations										
	161	6	162	5	160,b	3				
	110,b	10	139	0+	115,b	8				
			110,b	10						

(a) M = P,As

(b) Anion frequencies. Solid KPF_6: ν_1 751, ν_2 580, ν_3 830, ν_4 558, ν_5 477; G. M. Begun and A. C. Rutenberg, Inorg. Chem., 1967, 6, 2212. See also Table 2, Footnote (b).

(c) Obscured by anion feature.

TABLE 7

Vibrational Assignment for $[XeF_5^+F^-]_4$

$[XeF_5^+F^-]_4$							$Xe_2F_{11}^+$ in HF solution			XeF_5^+ in solid $[XeF_5^+][BF_4^-]$				Assignment (based on XeF_5^+)
Solid xenon hexafluoride				Liquid xenon hexafluoride (54°C)										
Raman		Infrared		Raman[a]			Raman			Raman		Infrared		
cm^{-1}	Rel.Int.	cm^{-1}	Rel.Int.	cm^{-1}	pol.	Rel.Int.	cm^{-1}	pol.	Rel.Int.	cm^{-1}	Rel.Int.	cm^{-1}	Rel.Int.	
656	vs			654	p	vs	667,b	p	100	667	65	672	ms	ν XeF_{ax}
636	vs	653	vs	637	dp	sh				673 654	19 5	650	s	ν_{deg} XeF_4
583	s	583	w	585	p	s	605,b	p	85	614	100			ν_s XeF_4
				576	dp	m	~590,b,sh	dp	~10					ν_{asym} XeF_4
404	vw			403	dp	w	410,b	dp	5	416 409	4 4			δ F_4XeF
				370	p?	w	360,b	p	7					δ_s XeF_4
300	w			295		w	302	p?	6	302	7			
204	vw			205		vw	214,b	dp	0+	219	0+			δ_{as} XeF_4
				95		mw								?

(a) Data from Reference 13.

TABLE 8

Raman Spectra of Solutions of Xenon Hexafluoride in WF_6

Liquid xenon hexafluoride (92°C)[a]			Gaseous xenon hexafluoride (85°C)[b]			Xenon hexafluoride in WF_6 solution (25°C)[c]									Assignment
						$XeF_6:WF_6$ = 1:5[d]			$XeF_6:WF_6$ = 1:10[d]			$XeF_6:WF_6$ = 1:40[d]			
cm^{-1}	pol.	Rel.Int.	cm^{-1}	pol.	Rel.Int.	cm^{-1}	pol.	Rel.Int.	cm^{-1}	pol.	Rel.Int.	cm^{-1}	pol.	Rel.Int.	
650[e]	p	s				652,sp	p	100	652,sp	p	100	652,sp	p	40	$[XeF_5^+F^-]_4$
						638,sh	dp	~10	638,sh	dp	~10	~640,sh	dp	~5	$[XeF_5^+F^-]_4$
616	p	sh	608 588	p	s	624	p	~ 5	622,sh	p	~15	621	p	60	XeF_6
577[e]						585	p	30	585	p	30	585	p	10	$[XeF_5^+F^-]_4$
						573,sh	dp	~ 5	573,sh	dp	~ 6	572	dp	2	$[XeF_5^+F^-]_4$
												~558	dp	2	XeF_4
506	dp	m	513	dp	s	507,b	dp	7	508,b	dp	16	508	dp	40	XeF_6
403	dp	w				404	dp	0+							$[XeF_5^+F^-]_4$
370	p	w				~370,b	p	1	~370,b	p	1		(f)		$[XeF_5^+F^-]_4$
295	p?	mw					(f)			(f)			(f)		$[XeF_5^+F^-]_4$
205	dp	vw				~200,b	dp	0+	~200,b	dp	0+				$[XeF_5^+F^-]_4$
												140,vb	dp	0+	XeF_6?
95	dp	w				~100,b	dp	0+							$[XeF_5^+F^-]_4$
			56	?	w										XeF_6

(a) Excited at 4358 Å; Reference 13.

(b) Excited at 6471 Å; Reference 14.

(c) Excited at 6471 Å; this work.

(d) Mole ratios.

(e) Depolarized shoulder on low-frequency side of peak.

(f) Region obscured by solvent.

TABLE 9

Raman spectra of xenon hexafluoride in HF solution[a]

XeF_6:HF = 1:10[b]			XeF_6:HF = 1:20[b]			XeF_6:HF = 1:150[b]			Assignment
cm^{-1}	pol.	Rel.Int.	cm^{-1}	pol.	Rel.Int.	cm^{-1}	pol.	Rel.Int.	
						672	p	s	XeF_5^+
			662,b	p	s	660,sh	p	m	$Xe_2F_{11}^+$
658	p	vs							$[XeF_5^+F^-]_4$
~640,sh	dp	w							$[XeF_5^+F^-]_4$
			621,sh	p	vvw	621	p	vs	XeF_5^+
			601	p	s	605,sh	p	m	$Xe_2F_{11}^+$
595	p	s							$[XeF_5^+F^-]_4$
580,sh	dp	w	585	dp	sh				$Xe_2F_{11}^+$, $[XeF_5^+F^-]_4$
510,sh	dp	vw							XeF_6
407	dp	w	410	dp	vw	408	dp	w	XeF_5^+, $Xe_2F_{11}^+$, $[XeF_5^+F^-]_4$
358	p	mw	360	p	mw	360	p	w	$Xe_2F_{11}^+$, $[XeF_5^+F^-]_4$
~210,b	dp	w	~210	dp	w	~200,b	dp	w	XeF_5^+, $Xe_2F_{11}^+$, $[XeF_5^+F^-]_4$

(a) Excited at 4880 Å.

(b) Mole ratios.

This report was done with support from the Department of Energy. Any conclusions or opinions expressed in this report represent solely those of the author(s) and not necessarily those of The Regents of the University of California, the Lawrence Berkeley Laboratory or the Department of Energy.

TECHNICAL INFORMATION DEPARTMENT
LAWRENCE BERKELEY LABORATORY
UNIVERSITY OF CALIFORNIA
BERKELEY, CALIFORNIA 94720